A generalised Monkman-Grant relation for creep life prediction: An application to 1CrMoV rotor steel

M. EVANS
School of Engineering, University of Wales Swansea, Singleton Park, Swansea, SA2 8PP, UK
E-mail: m.evans@swansea.ac.uk

Published online: 12 April 2006

A generalised Monkman—Grant relation, which can be derived from the 4-Θ projection technique, is proposed and then used to predict creep properties at non accelerated test conditions. In this generalisation, creep rates at low strains are used to predict minimum creep rates that are then used in the Monkman-Grant relation to predict times to failure. Predictions of creep properties for 1CrMoV from this generalisation and from the 4-Θ projection technique were assessed using the mean absolute percentage error (MAPE) and mean square error (MSE)—which was further decomposed into systematic and random components. When considering the accuracy with which minimum creep rates were predicted, all but the generalised Monkman-Grant relation using 0.1% strain had a lower MAPE compared to the 4-Θprojection technique. The generalised Monkman-Grant relation using 0.5% and 1% strains had larger random components of the MSE compared to the 4-Θprojection technique. When considering the accuracy with which times to failure were predicted, all of the generalised Monkman-Grant relations produced lower MAPE compared to the 4-Θ projection technique. However, only when creep rates were measured at 0.2% strain, did the generalised Monkman-Grant relation produce prediction errors that had a significantly higher random component. © *2006 Springer Science + Business Media, Inc.*

1. Introduction

Evans [1] has reviewed a number of creep property prediction models that have been used in the recent past. The most successful of these include the 4-Θ and 6-θ projection techniques developed and applied by Evans [2, 3] and Evans and Scharning [4], the continuum damage techniques (CDM) developed by Kachanov [5], Rabotnov [6] and latter generalised by Othman and Hayhurst [7] and the Ω methodology for the life assessment of components recently proposed by Prager [8]. What all these techniques have in common is the need to model the whole creep curve using some specified non linear function in time. The parameters of this functional relationship then require estimation using quite complicated non linear least squares procedures. This complication has limited the extent to which these relatively successful techniques have been implemented and applied within industry.

When attempting to predict creep life, engineers face a variety of complex problems including stress triaxility at stress inducing features, selection of hardening rules to be applied for relaxing of cyclical loading and the selection of suitable models for creep damage accumulation. Whilst these issues are undoubtedly important, this paper concentrates on projection techniques suitable for analyzing the results from uniaxial constant stress tests.

In particular, the objectives of this paper are to first demonstrate that a simple but generalised Monkman-Grant type relation can be derived from the 4-Θ projection technique which can be applied without the use of complicated non linear least squares techniques (which is central to the 4-Θ projection technique). Then the predictive capability of this generalised Monkman-Grant relation is assessed and compared to the 4-Θ projection technique using a number of capability statistics not typically used in the field of creep.

2. Experimental procedures

The Interdisciplinary Research Centre at Swansea (IRC) carries out high temperature testing programs involving many different materials. The test matrices are such that specimens are tested at highly accelerated stress conditions, i.e. at stresses well in excess of the design stress for such materials, but at close to operating temperatures. Further, all the tests are at constant stress and strain measurements are taken at regular time intervals so that detailed experimental creep curves are available.

0022-2461 © *2006 Springer Science + Business Media, Inc.*
DOI: 10.1007/s10853-005-5506-7

The batch of material tested at the IRC and used for the present investigation represents the lower bound creep strength properties anticipated for 1CrMoV rotor steels. The chemical composition of this batch of material (in wt%) was determined as 0.27% C, 0.22% Si, 0.77% Mn, 0.008% S, 0.015% P, 0.97% Cr, 0.76% Ni, 0.85% Mo, 0.39% V, 0.125% Cu, 0.008% Al and 0.017% Sn. Following oil quenching from 1238 K and tempering at 973 K, the material had a tensile strength of 741 MPa (at room temperature), elongation of 17%, reduction in area of 55% and a 0.2% proof stress of 618 MPa.

Eighteen test pieces, with a gauge length of 25.4 mm and a diameter of 3.8 mm, were tested in tension over a range of stresses at 783, 823 and 863 K using high precision constant-stress machines [9]. At 783 K, six specimens were placed on test over the stress range 425 to 290 MPa, at 823 K seven specimens were placed on test over the stress range 335 to 230 MPa and at 863 K six specimens were tested over the stress range 250 to 165 MPa. Up to 400 creep strain/time readings were taken during each of these tests. Normal creep curves were observed under all these test conditions. Table Ia shows the times to failure, minimum creep rates and creep rates at p (where p is in %) strain for all tested specimens. Creep rates were measured from the data points making up the experimental creep curves using numerical derivates (i.e. a second order version of a lagrange interpolating polynomial).

To assess the extrapolative capability of these models, long-term property data was supplied independently by an industrial consortium involving GEC-Alstom, Babcocks Energy, National Power, PowerGen and Nuclear Electric. These longer-term properties came from the same batch of material used in the accelerated test programme described above but for specimens with gauge lengths of 125 mm and diameters of 14 mm that were subjected to tests on high sensitivity constant-load tensile creep machines. Twelve specimens were tested in this way at 823 K and at stresses ranging from 215 to 77 MPa.

This longer-term data was published by Wilshire *et al.* [10] and at the time of publication in 1993 the creep property measurements made on these 12 specimens were incomplete. Table Ib summarises the full results of this longer-term data set. As can be seen, at the very low stresses only the times to low strains and creep rates at low strains were recorded (as these specimens had not failed when this data was published). Again creep rates were measured from the strain-time measurements made at p strain using numerical derivatives (i.e. a second order version of a lagrange interpolating polynomial). Unlike the short term data, all of these longer-term tests were carried out at constant load. The extent to which various creep property values are affected by the choice of constant load or constant stress methods depends on the material ductility and the shape of the creep curve. As shown by Wilshire *et al.* [10], the minimum creep rates were virtually unaffected, whereas only small reductions in creep lives were observed for constant load condition.

The short-term data set is therefore made up of $i = 1$ to N (where $N = 18$) specimens and the longer term data set is made up of $j = 1$ to M (where $M = 12$) specimens. In what follows j and i will now be used to represent the test condition at which the jth and ith specimens were tested. Predictions of minimum creep rates and times to failure using the 4-Θ projection technique are taken from Evans [11] and Table Ic presents some of these longer-term predictions.

3. Theoretical underpinnings of a generalised Monkman-Grant relation

3.1. The 4-Θ projection technique

The 4-Θ projection technique starts of by measuring complete creep curves at a variety of different accelerated test conditions, i.e. for all test conditions making up the short-term data set. Then each experimental creep curve is modeled using

$$\varepsilon_{i,t} = \Theta_{i,1}(1 - e^{-\Theta_{i,2}t}) + \Theta_{i,3}(e^{\Theta_{i,4}t} - 1) \qquad (1a)$$

where $\varepsilon_{i,t}$ is the strain at time t at accelerated test condition i. The parameters $\Theta_{i,1}$ to $\Theta_{i,4}$ are estimated using quite complicated non linear least squares algorithms.

To predict the creep curve at or close to operating test conditions, these estimated theta parameters are then related to the accelerated test conditions through the extrapolation function given by

$$\ln[\Theta_{i,k}] = \beta_{k,0} + \beta_{k,1}\tau_i + \beta_{k,2}T_i + \beta_{k,3}\tau_i T_i \qquad (1b)$$

where τ_i is the stress at accelerated test condition i and T_i is the temperature at the same test condition. With four Theta parameters, k varies from 1 to 4. Values for the $\beta_{k,l}$ parameters are estimated using complex weighted least squares procedures using only the accelerated test data. Weighting is required to deal with the fact that some of the Theta parameters are estimated with more reliability than others—depending on the experimental scatter in the measured creep curve.

Equation 1b is then used to predict the Theta values associated with operating condition j, $\Theta_{j,k}$. These are then substituted into Equation 1a to predict the shape of the creep curve at this operating condition. From this creep curve a range of creep properties can be read off. Evans [2] explains in detail how minimum creep rates, times to failure and times to various strains can be read off from the predicted creep curve.

A procedure not normally used in the theta projection technique is to use the Monkman-Grant relation [12] to obtain a life time prediction

$$\ln(t_{j,f}) = \lambda_0 + \lambda_1 \ln(\dot{\varepsilon}_{j,m}) \qquad (2)$$

where values for λ_0 and λ_1 are estimated using linear least squares from the accelerated test data only and $\dot{\varepsilon}_{j,m}$ is read off the predicted creep curve. Whilst doubt has been expressed in the past by Dobes and Malicka [13] and

TABLE IA Results making up the shorter-term data set

Temp. (K)	Stress (MPa)	Creep rate (h^{-1}) at p strain					Failure time (h)	Min. creep rate (h^{-1})
		0.05%	0.1%	0.2%	0.5%	1%		
783	425	1.70E–2	1.45E–2	1.20E–2	6.88E–3	4.51E–3	14.06	4.18E–3
783	370	1.18E–3	1.04E–3	8.72E–4	3.83E–4	2.91E–4	180.99	2.80E–4
783	350	1.61E–3	1.30E–3	4.90E–4	1.82E–4	1.38E–4	218.28	1.37E–4
783	320	5.94E–4	5.08E–4	2.44E–4	1.13E–4	8.81E–5	387.81	8.88E–5
783	305	1.29E–4	1.10E–4	7.89E–5	3.16E–5	3.21E–5	1469.89	2.77E–5
783	290	9.26E–5	5.43E–5	3.18E–5	1.41E–5	1.39E–5	4458.61	1.28E–5
823	335	1.11E–2	9.41E–3	8.17E–3	3.88E–3	2.63E–3	30.55	2.55E–3
823	310	6.35E–3	6.00E–3	3.92E–3	9.77E–4	7.18E–4	67.46	6.55E–4
823	290	5.10E–3	4.53E–3	2.33E–3	1.05E–3	7.56E–4	68.00	7.74E–4
823	270	6.24E–4	5.93E–4	4.91E–4	3.99E–4	2.27E–4	343.18	2.10E–4
823	250	8.58E–4	5.24E–4	2.98E–4	1.79E–4	1.05E–4	847.41	8.05E–5
823	240	7.02E–4	5.78E–4	4.73E–4	2.06E–4	1.04E–4	738.18	8.33E–5
823	230	4.40E–4	3.02E–4	1.25E–4	5.30E–5	3.26E–5	2583.93	2.63E–5
863	250	4.15E–2	7.24E–3	4.87E–3	2.98E–3	2.02E–3	39.88	1.77E–3
863	240	1.00E–2	8.26E–3	6.59E–3	3.83E–3	2.55E–3	36.95	1.95E–3
863	220	4.66E–3	4.16E–3	3.59E–3	1.56E–3	9.33E–4	127.64	7.12E–4
863	200	1.19E–3	9.91E–4	4.93E–4	3.27E–4	2.17E–4	300.15	1.90E–4
863	180	6.70E–4	6.22E–4	3.88E–4	1.53E–4	9.83E–5	573.82	9.06E–5
863	165	7.20E–4	6.68E–4	5.78E–4	1.89E–4	7.40E–5	1433.8	4.10E-5

Creep rates at p strain were measured from the data points making up the experimental creep curves using a second order version of a lagrange interpolating polynomial.

TABLE IB Results making up the longer-term data set

Stress (MPa)	Creep rate (h^{-1}) at p strain					Failure time (h)	Rupture elongation (%)	Min. creep rate (h^{-1})
	0.05%	0.1%	0.2%	0.5%	1%			
215	–	–	–	–	–	1359	27.2	–
185	–	–	–	–	–	2956	21.7	–
185	–	–	–	–	–	3660	19.6	–
170	–	–	–	–	–	8623	22.0	–
170	–	9.2E–5	2.0E–5	4.6E–6	1.7E–6	13559	15.4	2.5E–06
154	–	–	–	–	–	24328	15.5	–
139	4.4E–5	7.5E–6	4.0E–6	2.01E–6	1.2E–6	30558	15.1	1.1E–06
139	–	8.2E–6	4.0E–6	7.9E–7	–	–	–	–
139	–	1.1E–5	4.5E–6	9.8E–7	–	–	–	–
108	4.3E–6	9.0E–7	45E–7	2.5E–7	2.3E–7	–	–	2.1E–07
77	1.5E–6	2.2E–7	1.0E–7	5.6E–8	–	–	–	–
77	1.6E–6	1.8E–7	7.7E–8	–	–	–	–	4.0E–08

– No observation made. Creep rates at p strain were measured from the strain-time measurements made at p strain using a second order version of a lagrange interpolating polynomial.

Evans [14] as to whether the parameters of the Monkman-Grant relation are constant over all temperatures, Evans [15] has shown that these parameters are constant over a very wide range of stresses and at all temperatures below 873 K (this assertion is limited to 2.25 CrMo material and work on long term data for other materials would be a beneficial area for future research).

3.2. The relationship between creep rates within the 4-Θ projection technique

The above 4-Θ projection technique implies an approximate linear dependence in a double logarithmic coordinate system between creep rates measured at any low strain and the minimum creep rate. Given the nature of Equation 1 above, this can not be shown algebraically in a closed form expression. However, the $\beta_{k,1}$ values shown in Table II were used in conjunction with Equation 1b to

TABLE IC Longer-term predictions made using the 4-Θ projection technique at 823 K

Stress (MPa)	Predicted Failure time (h)	Predicted Minimum creep rate (h^{-1})
215	3,126	1.9E–5
185	10,599	5.1E–6
170	19,505	2.6E–6
154	35,879	1.4E–6
139	65,974	7.2E–7
108	222,864	1.9E–7
77	752,147	4.2E–8

TABLE II The β parameters of Equation 1b use to simulate $\Theta_{i,k}$ values in the 4-Θ projection technique

	$\beta_{k,0}$	$\beta_{k,1}$	$\beta_{k,2}$	$\beta_{k,3}$
$k = 1$	0.25058	−0.023321	−0.003906	2.34E-05
$k = 2$	−95.97042	0.062727	0.086519	−1.89E-05
$k = 3$	−1.855094	−0.039266	−0.005962	5.53E-05
$k = 4$	−77.03491	0.013713	0.065145	3.12E-05

calculate $\Theta_{i,k}$ values over a very wide range of stresses and temperatures. (These $\beta_{k,l}$ values are actually the estimates obtained from the short-term data base described in Section 2 above). Stresses ranged from 500 down to 50 MPa and temperatures from 923 down to 723 K. These $\Theta_{i,k}$ values were then used to calculate minimum creep rates and creep rates at various strains (through the differentiation of Equation 1a).

It can be seen from Fig. 1 that on a double logarithmic coordinate system there is a very good linear relationship existing between the minimum creep rate and the creep rate at p strain within the 4-Θ projection technique. This relationship does however change with the strain chosen—with the intercept term increasing with increasing strain.

3.3. The generalised Monkman-Grant relation

Fig. 1 suggests a simple approach to predicting minimum creep rates at close to operating conditions. There is no need to measure complete creep curves, or from them the theta values at various accelerated test conditions. Nor is there a need to extrapolate these theta values. Instead, N specimens are tested under accelerated conditions until failure. For each specimen, the minimum creep rate is measured together with the creep rates at various low strains (typically 0.05% through to 1%) and the times to failure. From this data the following relationship is then estimated using linear least squares

$$\ln(\dot{\varepsilon}_{i,m}) = \delta_0 + \delta_1 \ln(\dot{\varepsilon}_{i,p}) \tag{3a}$$

where $\dot{\varepsilon}_{i,p}$is the creep rate at p creep strain under accelerated test condition i. To predict minimum creep rates around operating conditions (test condition j), M specimens are tested under these conditions until p strain has been reached. These M tests are then discontinued. The measured creep rates at p strain, $\dot{\varepsilon}_{j,p}$, are then inserted into Equation 3a to predict the minimum creep rate

$$\ln(\dot{\varepsilon}_{j,m}) = \delta_0 + \delta_1 \ln(\dot{\varepsilon}_{j,p}) \tag{3b}$$

The time to failure around operating conditions can in turn be predicted using a generalised Monkman-Grant relation which is obtained by substituting Eqs. 3b into Equation 2

$$\ln(t_{j,f}) = \phi_0 + \phi_1 \ln(\dot{\varepsilon}_{j,m}) \tag{3c}$$

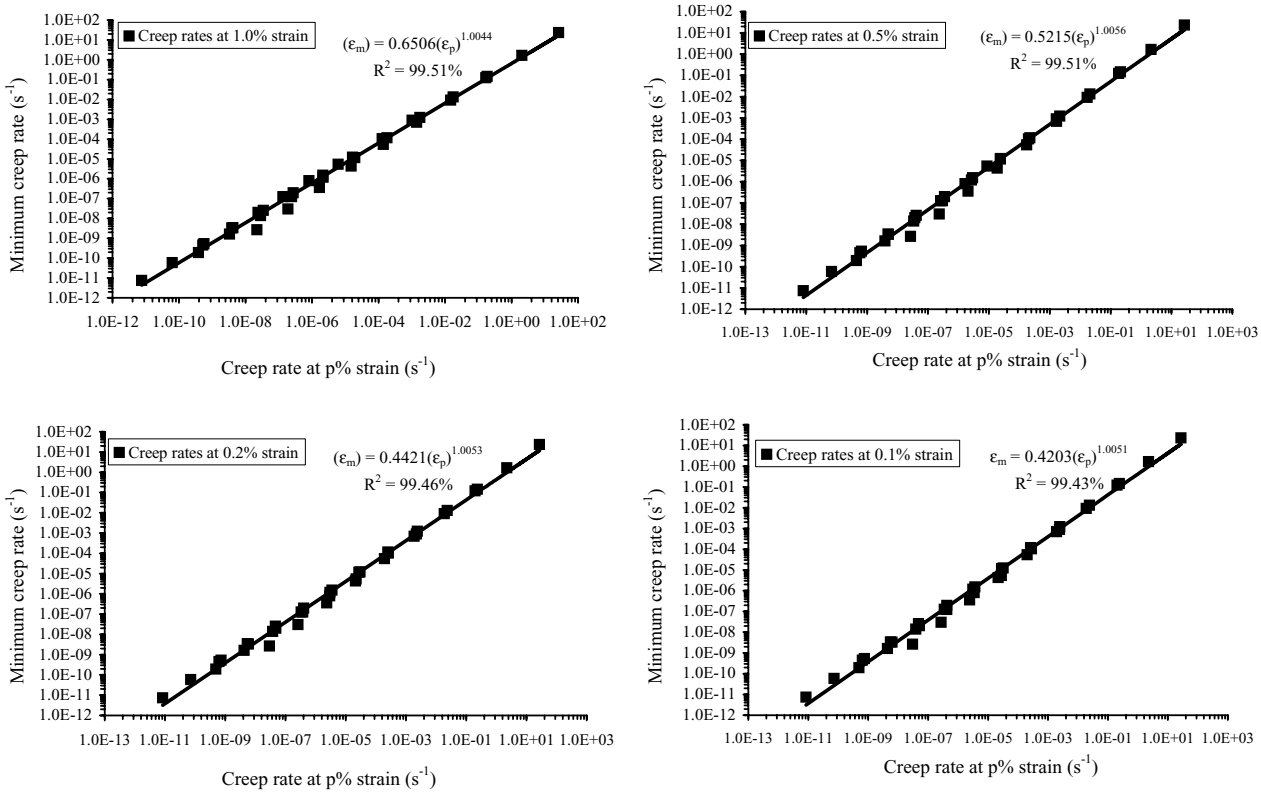

Figure 1 The relationship between minimum creep rate and creep rate at p strain implied by the 4-Θ projection technique.

where $\phi_0 = \lambda_0 + \lambda_1\delta_0$ and $\phi_1 = \lambda_1\delta_1$. In all cases the values for λ and δ are estimated only from the accelerated or short-term data set.

The standard Monkman-Grant relation has the advantage of being easy to estimate and once the minimum creep rate is known, the life of the material can be predicted from it using Equation 2. This is attractive because specimens can be put on test at operating conditions until the minimum creep rate is recorded and then removed. Because this typically occurs well before the materials life, a life prediction can be made well in advance of failure. The disadvantage of using the standard Monkman-Grant relation to predict safe life is that at operating conditions, it can still take tens of thousands of hours to reach the minimum creep rate and tests of this length are often not viable from a practical or economic perspective. The generalised Monkman-Grant relation described in Equation 3c overcomes this limitation because creep rates at very low strains are observed well before the minimum creep rate.

4. Predictive capability

To assess the predictive accuracy of the creep property prediction models described above, these models are first estimated using the results from the N specimens making up the short-term data set. The models are then used to predict the properties of those M specimens tested in the longer-term data set. One simple measure of predictive accuracy is the mean squared prediction error (MSE) or the mean absolute prediction error (MAE). Often the MSE is square rooted to be in the same units as Y_j

$$MSE = \frac{1}{M}\sum_{j=1}^{M}\left[Y_j - \hat{Y}_j\right]^2 \tag{4a}$$

$$MAE = \frac{1}{M}\sum_{j=1}^{M}\left[\left|Y_j - \hat{Y}_j\right|\right] \tag{4b}$$

where $\hat{Y}_j$ is the predicted creep property for the specimen tested at the jth longer-term test condition and Y_j is the actual creep property for this specimen (squares or absolute errors are used so that over and underestimates are not offsetting in the averaging procedure). However, both the MSE and the MAE lack any sense of scale and this can be overcome by expressing the prediction error as a percentage of the actual value

$$MSPE = \frac{100}{M}\sum_{j=1}^{M}\left[\frac{(Y_j - \hat{Y}_j)}{Y_j}\right]^2 \tag{4c}$$

$$MAPE = \frac{100}{M}\sum_{j=1}^{M}\left[\left|\frac{Y_j - \hat{Y}_j}{Y_j}\right|\right] \tag{4d}$$

The MSE is a useful way of assessing the predictive accuracy of a creep model because this error, following Theil's analysis [16], can be decomposed into a number of different components

$$MSE = \frac{1}{M}\sum_{j=1}^{M} e_j^2 = \frac{1}{M}\sum_{j=1}^{M}\left[(e_j - \bar{e}) + \bar{e}\right]^2$$

and upon expanding the brackets

$$MSE = \frac{\sum_{j=1}^{M}(e_j - \bar{e})^2}{M} + \bar{e}^2 + \frac{2e_i\sum_{j=1}^{M}(e_j - \bar{e})}{M} \tag{5a}$$

where $e_j = Y_j - \hat{Y}_j$ is the prediction error associated with the jth test condition in the longer-term data set and $\bar{e}$ is the average prediction error calculated from the M longer-term data points. The first expression in Equation 5a is the sample variance of the prediction error (biased in small samples), S_e^2, and for any sample the $(e - \bar{e})$ term always sums to zero so

$$MSE = \bar{e}^2 + S_e^2 \tag{5b}$$

A good model will predict with an average error close to zero and with only small over/under predictions around this average, i.e. small variation in the prediction error. A plot of actual versus predicted creep property values can be used to further decompose this MSE. On such a plot, all the data points should fall on a one to one line if the creep prediction model is a perfect predictor. That is $\alpha = 0$, $\beta = 1$ and $S_\varepsilon^2 = 0$ in

$$Y_j = \alpha + \beta\hat{Y}_j + \varepsilon_j \tag{6}$$

where ε_j is the extent to which the jth creep property prediction differs from $\alpha + \beta\hat{Y}_j$, and S_ε^2 is the variance in such disturbances. Rearranging Equation 6 above for the prediction error gives

$$(Y_j - \hat{Y}_j) = e_j = \alpha + (\beta - 1)\hat{Y}_j + \varepsilon_i \tag{7}$$

Assuming that $\hat{Y}_i$ and ε_i are independent of each other it follows from Equations 7 and 5b that

$$\mathrm{MSE} = \bar{e}^2 + \left\{(\beta - 1)^2 S_{\hat{Y}}^2\right\} + S_\varepsilon^2 \tag{8a}$$

where $S_{\hat{Y}}^2$ is the variance of the predictions. Thus

$$\begin{aligned} 1 &= \frac{\bar{e}^2}{MSE} + \frac{\left\{(\beta - 1)^2 S_{\hat{Y}}^2\right\}}{MSE} + \frac{S_\varepsilon^2}{MSE} \\ &= U_\mathrm{M} + U_\mathrm{R} + U_\mathrm{D} \end{aligned} \tag{8b}$$

Equation 8b shows that a proportion of the MSE is due to the average of the models predictions differing from the average of the actual values U_M. Another part is due to the slope of the best fit line on the actual v prediction plot differing from 1, U_R. Both U_M and U_R therefore represent systematic errors and large values for these two terms suggest that the creep model is incomplete in some

way. For example, it may suggest that some explanatory variables are missing from the model, or that the models functional relationship between the creep property and test conditions is incorrect. A final part of the *MSE* is due to the data points on the actual v prediction plot not all lying on the best fit line, U_D. When they all lie on the best fit line $S_\varepsilon^2 = 0$. As the ε_i are random in nature, U_D represents random prediction errors that can't be reduced. Ideally, a creep property model should have a very small *MSE* with $U_M = U_R \cong 0$ and $1 \cong U_D$.

5. Creep property predictions using the traditional and simplified 4-Θ models

5.1. Predicting minimum creep rates

Fig. 2a shows the actual relationships existing between creep rates at various low strains and the minimum creep rate both in the short and longer-term data sets. At each chosen strain there is a clear linear correlation between the logarithmic creep rate at that strain and the logarithmic minimum creep rate within the short-term data set. For example, the logarithmic creep rate at 0.1% strain can explain 93.01% of the variation in the logarithmic minimum creep rate in the short-term data set. This rises to 99.3% when using the creep rate at 1% strain. At all strains the value for δ_1 in Equation 3a appears to fluctuate randomly around a value of unity. However, δ_0 appears to increase with increasing strain and these two results are consistent with that to be expected from the 4-Θ projection technique.

Fig. 2a also shows that at all strains, a reasonable prediction of the minimum creep rate in the longer-term data set can be made. The accuracy of these predictions are quantified in Table III where the MAPE and the *MSE* together with its decomposition (given by Equation 8b) are shown. The 4-Θ projection technique produced a *MAPE* of just 47.37%. Further, the majority of the errors made in predicting the minimum creep rate in this way were not random in nature. These systematic errors made in predicting the minimum creep rate amounted to 92.51%, with 30.57% of the *MSE* attributable to the average of the models predictions differing from the average of the actual values and 61.94% of the *MSE* attributable to the slope of the best fit line on the actual v prediction plot differing from unity. Only 7.49% of the prediction errors were random in nature.

In contrast to this, the best of the generalised Monkman-Grant relations (based on the MAPE) used the creep rates at 0.5% and 1.0% strains. For example, using creep rates at 0.5% strain the majority of the errors made in predicting the minimum creep rate are now random in nature (52.8%). The systematic errors made in predicting the minimum creep rate amounted to 47.2%, with 1.07% of the MSE attributable to the average of the models predictions differing from the average of the actual values and 46.13% of the MSE attributable to the slope of the best fit line on the actual v prediction plot differing from 1. Indeed both these models perform much better than the 4-Θ projection technique.

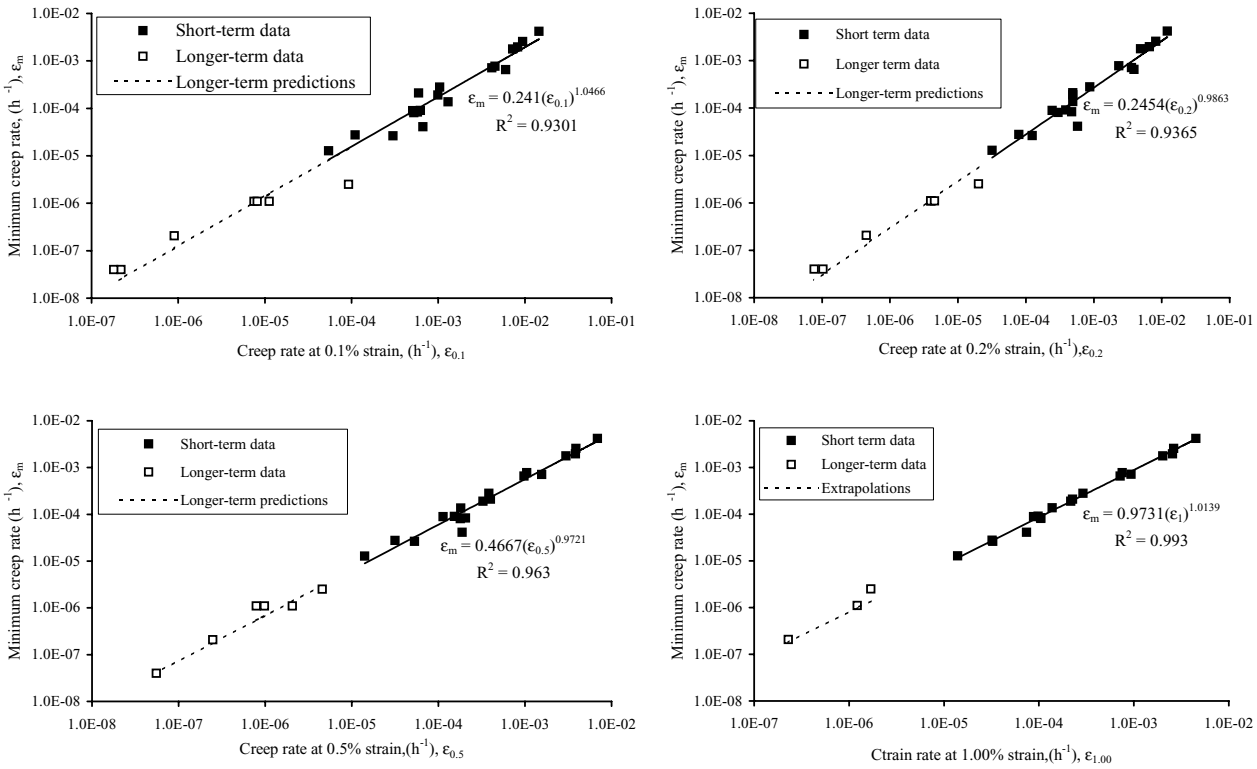

(a)

Figure 2 (a) The observed experimental relationship between minimum creep rate and creep rate at p strain. (b) The observed experimental relationship between failure time and creep rate at p strain.

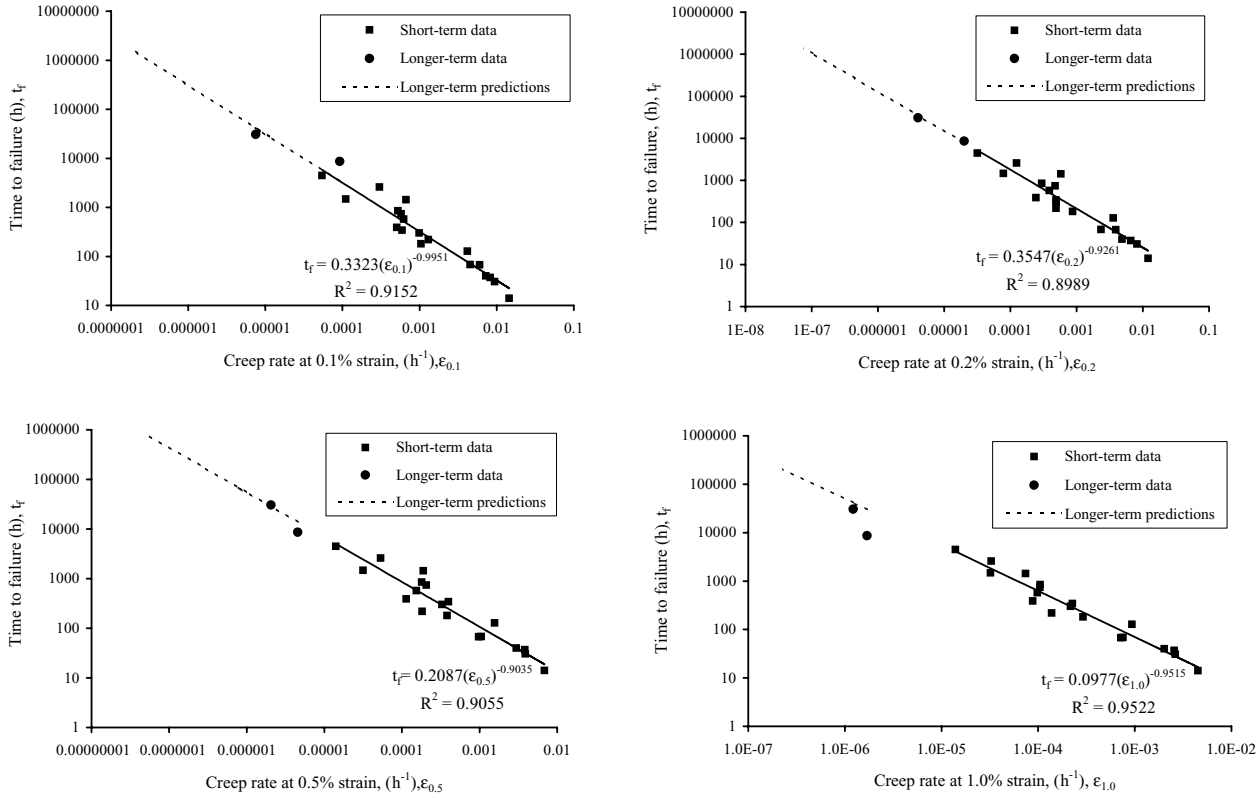

(b)

Figure 2 Continued.

Even when creep rates at lower strains are used, the models perform reasonable well with acceptable *MAPE*, although the majority of the errors made in predicting the minimum creep rate are then systematic in nature. This may reflect the larger errors made in measuring creep rates very early on in a creep curves evolution. What stands out from this is that the extra complexity involved with using the 4-Θ projection technique as compared to the generalised Monkman-Grant relations does not reflect itself in a proportionate improvement in predictive accuracy. However, there remains the question of which level of strain to measure the creep rate. A future paper will address this issue further by assessing whether a combination of strains is best.

5.2. Predicting times to failure

Fig. 2b shows the actual relationship existing between the minimum creep rates at various low strains and time to failure both in the short and longer-term data sets. At each chosen strain there is a clear linear correlation between the logarithm of the creep rate at that strain and the logarithmic time to failure within the short-term data set. For example, the logarithmic creep rate at 0.1% strain can explain 91.52% of the variation in the logarithm of the time to failure in the short-term data set. This rises to 95.2% when using the creep rate at 1% strain. It can also be seen that the generalised Monkman-Grant relations shown Fig. 2b extrapolate well to the longer-term data even at low strains. This is because the R^2 values associated with the lowest strains do not appear to be very much lower than that associated with 1% strain or indeed the minimum creep rate over the short-term data. (The R^2 associated with the Monkman-Grant relation is 97%). At all strains the value for φ_1 in Equation 3c appears to fluctuate just below a value of unity. However, φ_0 appears to decrease with increasing strain.

TABLE III The MAPE, MSE and MSE decomposition for predictions of the minimum creep rate

Predictive statistics	Generalised Monkman-Grant models using creep rates at:				
	0.1% strain	0.2% strain	0.5% strain	1% strain	4-Θ
MAPE	94.25%	36.76%	25.40%	22.90%	47.37%
MSE	2.04E–11	1.49E–12	1.36E–13	4.30E–13	3.36E–13
U_M	15.12%	16.48%	1.07%	41.79%	30.57%
U_R	84.14%	79.06%	46.13%	36.75%	61.94%
U_D	0.74%	4.46%	52.80%	21.46%	7.49%

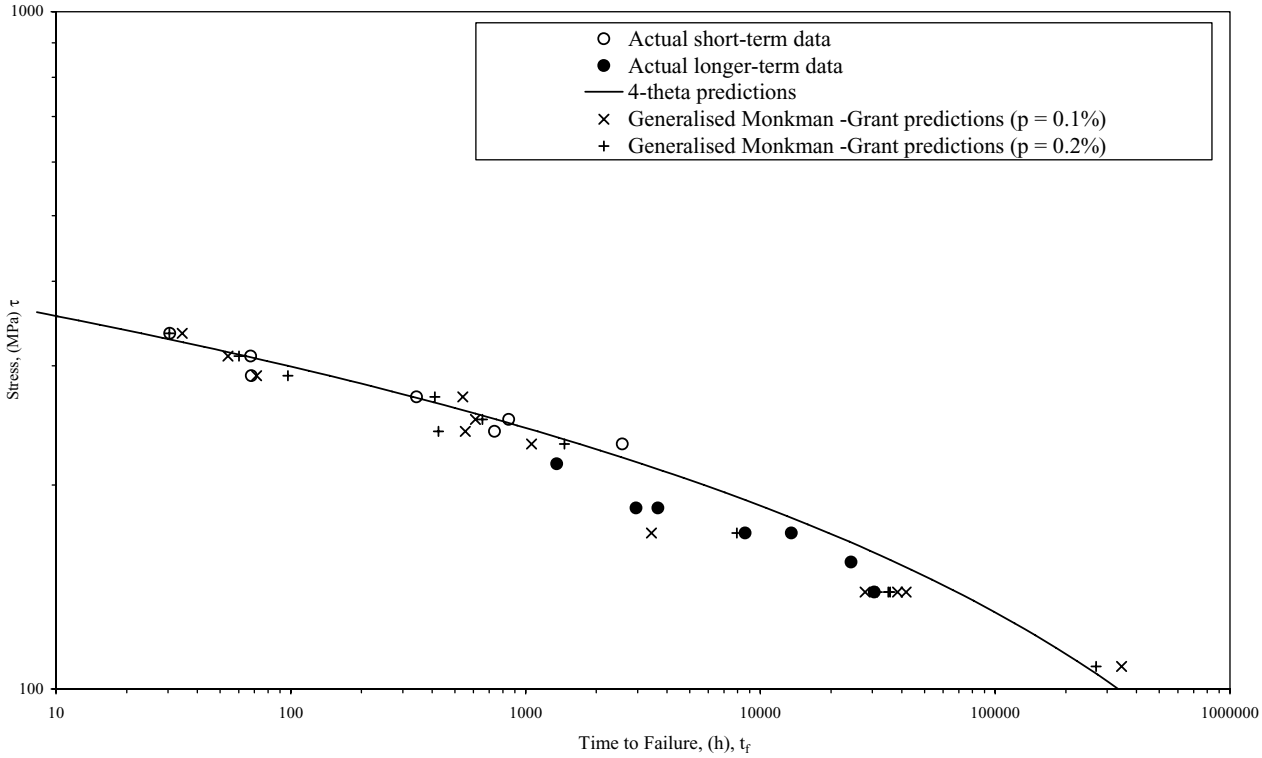

Figure 3 Predicted $\ln(\tau)/\ln(t_f)$ plots for constant stress conditions, compared with the measured t_f values obtained from short-term constant-st 823 K.

Fig. 3 gives a slightly different perspective on the short and longer-term predictions shown in Fig. 2b. In Fig. 3 the actual times to failure, predicted times to failure associated with the generalised Monkman-Grant relation (with creep rates measured at 0.1 and 0.2% strain) and predicted times to failure given by the 4-Θ projection technique at 823 K are plotted against various stresses. All these procedures produce good predictions of the short term data, but the generalised Monkman-Grant relation does not overestimate the longer-term data to the same extent as the 4-Θ projection technique. (Note how only the 4-Θ projection technique produces predictions that are a smooth function of stress).

Table IV further quantifies the accuracy of the projections shown in Figures 2b and 3 using the *MAPE* and the *MSE* associated with the predicted times to failure. Also shown for each of these predictions is a decomposition of the *MSE* using Equation 8b above. The 4-Θ projection technique produced a *MAPE* of just over 100%. Further, the majority of the errors made in predicting the times to failure were systematic in nature. For example, around 81% of the *MSE* is attributable to the average of the models predictions differing from the average of the actual values. Around 14% of the *MSE* was random in composition. In contrast, the best of the generalised Monkman-Grant relations used the creep rate measured at 0.2%. This model produced a *MAPE* of around 18%. However, the majority of the errors made in predicting the times to failure were again systematic in nature. Around 77% of the *MSE* is attributable to the average of the models predictions differing from the average of the actual values and around 22% of the MSE was random in composition.

The predictive capability of the other generalised Monkman-Grant relations models were not so good as the one above. This again raises the question of which strain to use. It may be possible to combine the predictions from all the generalised Monkman-Grant relations models into a single improved prediction of time to failure. This issue on combinations of forecasts will be addressed in a future paper.

TABLE IV The MAPE, MSE and MSE decomposition for predictions of the time to failure

Predictive statistics	Generalised Monkman-Grant models using creep rates at:				
	0.1% strain	0.2% strain	0.5% strain	1% strain	4-Θ
MAPE	40.35%	18.39%	66.44%	103.37%	103.54%
MSE	5.77E+7	7.75E+8	2.16E+10	1.5E+9	2.76E+9
U_M	0.28%	76.91%	72.14%	97.88%	81.24%
U_R	83.67%	1.38%	17.53%	1.64%	4.73%
U_D	16.06%	21.71%	10.33%	0.48%	14.02%

The poorer performance (based on the MAPE) of the 4-Θ projection technique relative to most of the generalised Monkman-Grant relations probably reflect the poorer performance of the 4-Θ projection technique in predicting minimum creep rates. This in turn may be the result of obtaining a good fit to the tertiary part of the creep curve in the 4-Θ projection technique.

Finally, it can be noted from Tables III and IV that the *MSE* and the *MAPE* give slightly different rankings of all the different approaches described above. When ranking techniques in this way it is always best to use the *MAPE* because, unlike the *MSE*, it scales the prediction error relative to the actual value. Further, the *MSE* can be distorted by a few large prediction errors as a result of the squaring procedure—a problem avoided through the use of absolute values. The *MSE* is useful only because it can be easily decomposed into a systematic and random component (in a way that the *MAPE* can't). As an absolute measure of predictive accuracy it can be misleading.

6. Conclusion

It has been demonstrated, using simple simulations, that a linear dependence in a double logarithmic coordinate system exists between creep rates measured at any low strain and the minimum creep rate if creep obeys the equations making up the 4-Θ projection technique. This provides for the possibility of modelling creep properties using generalised Monkman-Grant relations—that differ only by the low strain chosen to measure the creep rate which is used to predict the minimum creep rate. Short-term experimental data confirms that such a relationship does indeed appear to exist. Further, this relationship also holds into the longer-term data so that the generalised Monkman-Grant relation produces good predictions of the minimum creep rates observed in the longer-term data. Indeed, all but the generalised Monkman-Grant relation using 0.1% strain had a lower *MAPE* compared to the 4-Θprojection technique. The generalised Monkman-Grant relation using 0.5 and 1% strains had larger random components of the *MSE* compared to the 4-Θprojection technique (and a very similar random component at 0.2%).

When considering the accuracy with which times to failure were predicted all of the generalised Monkman-Grant relations produced lower *MAPE* compared to the 4-Θ projection technique. However, only when creep rates were measured at 0.2% strain, did the generalised Monkman-Grant relation produce prediction errors that had a significantly higher random component compared to the traditional 4-Θ projection technique.

The predictive capability of some generalised Monkman-Grant relations were much better than others and so the question of at which strain should creep rates be measured appears again to be critical. It may be possible to combine the predictions from all the generalised Monkman-Grant relations into a single improved prediction of time to failure. This issue on combinations of forecasts will be addressed in a future paper.

References

1. M. EVANS, *J. Mater Sci.* **39** (2004) 2053.
2. R. W. EVANS, *Mat. Sci. Technol.* **5** (1989) 699.
3. *Idem. ibid.* **16** (2000) 6.
4. R. W. EVANS and P. J. SCHARNING, *Mat. Sci. Technol.*, **17** (2001) 487.
5. L. M. KACHANOV, "The Theory of Creep" (National Lending Library, Boston Spa, UK, 1967).
6. Y. N. RABOTNOV, "Creep Problems in Structural Members" (North Holland, Amsterdam, 1969).
7. A. M. OTHMAN and D. R. HAYHURST, *Int. J. Mech. Sci.* **32**(1) (1990) 35.
8. M. PRAGER, The Omega Method—An Engineering Approach to Life Assessment. *Journal of Pressure Vessels Technology* **122** (2000) 273.
9. R. W. EVANS and B. WILSHIRE, "Creep of Metals and Alloys" (The Institute of Materials, London, 1985).
10. R. W. EVANS, M. R. WILLIS, B. WILSHIRE, S. HOLDSWORTH, B. SENIOR, A. FLEMING, M. SPINDLER and J. A. WILLIAMS, in Proceedings of the 5th International Conference on "Creep and Fracture of Materials and Structures", Swansea, 1993, edited by B. Wilshire and R.W. Evans (The Institute of Materials, London, 1993) p. 633.
11. M. EVANS, *J. Mater Sci.* **35** (2000) 2937.
12. F. C. MONKMAN and N. J. GRANT, edited by N. J. Grant and A. W. Mullendore (MIT Press, Boston, 1963) vol. 56.
13. F. DOBES and K. MILICKA, *Met. Sci.* **10** (1976) 382.
14. M. EVANS, *Mater Sci. Technol.* **15** (1999) 91.
15. M. EVANS, in Proceeding of the International Conference on "Creep and Fracture in High Temperature Components—Design and Life Assessment Issues", London 2005, organized by the European Creep Collaborative Committee.
16. H. THEIL, "Applied Economic Forecasting" (Rand McNally & Company, 1966).

Received 6 June
and accepted 8 June 2005